

UC Irvine

UC Irvine Previously Published Works

Title

Synthesis of Pleuromutilin

Permalink

<https://escholarship.org/uc/item/9b12g5f3>

Journal

Journal of the American Chemical Society, 144(23)

ISSN

0002-7863

Authors

Foy, Nicholas J
Pronin, Sergey V

Publication Date

2022-06-15

DOI

10.1021/jacs.2c04708

Peer reviewed



HHS Public Access

Author manuscript

J Am Chem Soc. Author manuscript; available in PMC 2023 June 15.

Published in final edited form as:

J Am Chem Soc. 2022 June 15; 144(23): 10174–10179. doi:10.1021/jacs.2c04708.

Synthesis of Pleuromutilin

Nicholas J. Foy,

Department of Chemistry, University of California, Irvine, California 92697-2025, United States

Sergey V. Pronin

Department of Chemistry, University of California, Irvine, California 92697-2025, United States

Abstract

Synthesis of a potent inhibitor of bacterial protein synthesis, pleuromutilin, is described. Assembly of the critical cyclooctane fragment relies on an oxidative ring-expansion, and complete stereochemical relay in the synthetic sequence is enabled by the judicious choice of tactics. The requisite connectivity pattern of the perhydroindanone motif is rapidly established in a sequence of cycloaddition and radical cyclization events. Application of this strategy allows for preparation of the target natural product in 16 steps from commercially available material.

Pleuromutilin (**1**) is a terpenoid produced by basidiomycetes from the *Clitopilus* genus and discovered during the search for new fungal metabolites with antibacterial properties (Figure 1).¹ This natural product exhibits potent activity against Gram-positive pathogens, which results from binding to the bacterial ribosome at a highly conserved peptidyl transferase center.² The unique mechanism of action minimizes the appearance of resistant strains and ensures a lack of cross-resistance with other inhibitors of protein synthesis.^{3,4} Spectroscopic and degradation studies revealed a distinctive tricyclic motif of mutilin (**2**), which is found as a glycolate at C14 in pleuromutilin (**1**).^{5–7} The ester functionality is required for biological activity and has provided a crucial handle for structural modifications during the development of semisynthetic mutilin antibiotics.⁸ Initial efforts led to the identification of tiamulin and valnemulin for veterinary applications and retapamulin (**3**) for treatment of skin infections.⁹ Recent approval of lefamulin (**4**) for the treatment of community-acquired bacterial pneumonia marked the first successful development of a mutilin antibiotic for systemic administration in humans.¹⁰ Introduction of a substituted thioglycolate at C14 has been a hallmark of all compounds evaluated in clinical settings so far, with the remainder of

Corresponding Author: **Sergey V. Pronin** – *Department of Chemistry, University of California, Irvine, California 92697-2025, United States*; spronin@uci.edu.

ASSOCIATED CONTENT

Supporting Information

The Supporting Information is available free of charge at <https://pubs.acs.org/doi/10.1021/jacs.2c04708>.

Experimental and computational procedures and characterization data for all new compounds (PDF)

Accession Codes

CCDC 2170014–2170016 contain the supplementary crystallographic data for this paper. These data can be obtained free of charge via www.ccdc.cam.ac.uk/data_request/cif, or by emailing data_request@ccdc.cam.ac.uk, or by contacting The Cambridge Crystallographic Data Centre, 12 Union Road, Cambridge CB2 1EZ, UK; fax: +44 1223 336033.

Complete contact information is available at: <https://pubs.acs.org/10.1021/jacs.2c04708>

The authors declare no competing financial interest.

the scaffold unchanged.¹¹ Modifications of the terpenoid core present a challenge due to its complex reactivity patterns. Nevertheless, new derivatives of 12-*epi*-mutilin show promise in extending the spectrum of antibacterial activity to Gram-negative pathogens.¹²

The combination of structural features and promising biological activity has prompted multiple investigations into the chemical synthesis of mutilin antibiotics.^{13,14} These efforts led to identification of several strategic bonds within the terpenoid core and ultimately resulted in a diverse collection of synthetic sequences to access the target compounds. Here, we demonstrate a new approach to these antibacterial agents that permits rapid construction of the unique tricyclic framework with robust stereochemical relay throughout the synthetic sequence. Application of our strategy has secured access to mutilin (**2**) and pleuromutilin (**1**) in 15 and 16 steps, respectively, from commercially available material.

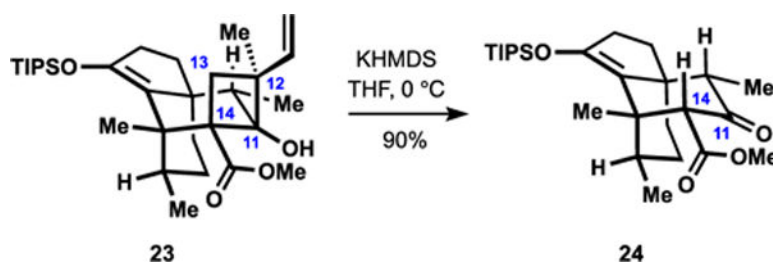
Our approach to the terpenoid core of mutilin antibiotics relied on ring-expansion of a six-membered carbocyclic fragment to access the desired cyclooctane motif (Figure 1). To accomplish the required insertion of one isoprene unit, we envisioned an annulation to form the C11–C12 and C13–C14 bonds in a fused ring system, which was expected to undergo oxidative cleavage of the C11–C14 bond and furnish the desired functionalization pattern. We also anticipated that a rapid assembly of the requisite precursor to ring-expansion would be enabled by a cycloaddition to form the C4–C5 and C9–C10 bonds and a radical cyclization to form the C5–C6 bond. Notably, the presence of ketones at C3 and C11 in the structure of intermediates was expected to allow for epimerization of critical stereocenters at C4 and C10 when found necessary for the success of the synthesis.¹⁵

Our synthesis began with Diels–Alder cycloaddition of cyclopentenone **5** and siloxydiene **6** (Scheme 1). We identified a combination of methylaluminum triflimide and a silyl triflate as the only competent catalytic system among the evaluated Lewis acids.^{16,17} Tetrahydroindanone **7** was formed as a major product, along with the minor diastereomer resulting from *endo* approach in the cycloaddition.¹⁸ The observed *exo* selectivity is noteworthy, because the configuration at C10 proved critical to successful installation of the quaternary center at C12, whereas the stereocenter at C4 was ablated at the later stages (see below). Oxidation of enol ether **7** with CAN produced unsaturated ketone **8**.¹⁹ Subjection of diene **8** to the conditions of iron-catalyzed hydrogen atom transfer (HAT) resulted in formation of tricyclic motif **9**, presumably through selective generation of a secondary alkyl radical from the monosubstituted alkene and subsequent Giese addition to the pendant unsaturated ketone.^{20–23} Notably, construction of the C5–C6 bond proceeded with exceptional stereocontrol, delivering the desired scaffold as a single diastereomer in synthetically useful yield.²⁴ We found diene **8** to be the optimal precursor en route to the tricyclic motif. Substrates containing an additional electron-withdrawing group at C14 underwent cyclization with diminished diastereoselectivity, while introduction of other substituents at the same position resulted in significant reduction of efficiency.

Elaboration of tricyclic diketone **9** began with conversion of the cyclopentanone to the corresponding silyl enol ether and subsequent alkoxyacylation of the remaining ketone at the less substituted position (Scheme 2).²⁵ The choice of enoxysilane as a protecting group for the carbonyl at C3 enabled functionalization at C4 at a later point in the synthesis

and also established an optimal steric environment for alkylation of an enolate at C14. The ester at C14 proved critical to implementation of the planned ring-expansion and access to the desired functionalization pattern in the cyclooctane motif. Thus, introduction of the fused cyclobutane fragment was accomplished upon propargylation of an enolate of keto ester **10** with iodide **11** and reductive cyclization of the corresponding alkyne **12** to form allylic alcohol **13**.²⁶ We found that subjection of cyclobutanol **13** to basic conditions established an equilibrium with the corresponding retro-aldol product, which could be trapped as the isolable ketene silyl acetal **14** under carefully controlled conditions.²⁷ Further addition of base directly to the reaction mixture produced an extended enolate of unsaturated ketone **14**, and subsequent alkylation with methyl iodide established the desired quaternary center at C12. Notably, the alkylation proceeded in a highly diastereoselective manner, which we attribute to the effect of the stereochemical configuration at C10 on the conformation of the intermediate enolate. Our computational studies with related enol **21** and its diastereomer **22**, which is epimeric at C10, suggest opposing conformational preferences in these cyclooctene motifs (Figure 2). The computed structure **21** indicates a more sterically accessible face of the enol that is consistent with the stereochemical outcome observed in our alkylation of unsaturated ketone **14**, whereas epimeric structure **22** predicts undesired direction of electrophilic attack.²⁸ These results imply that the configuration at C10 obtained in the *exo*-selective cycloaddition may play an important role in the desired stereochemical relay during our assembly of the quaternary center at C12.

To our surprise, the ketene silyl acetal motif of intermediate **15** (see Scheme 2) proved resistant to oxidation, and efforts to install a carbonyl group at C14 led primarily to functionalization of the vinyl substituent. Furthermore, the corresponding enolate, generated upon treatment of ketene silyl acetal **15** with a source of fluoride, underwent rapid aldol cyclization to reestablish the cyclobutanol moiety, which precluded derivatization with added electrophilic reagents. In contrast to the aldol motif of intermediate **13**, the newly formed cyclobutanol containing a quaternary center at C12 did not engage in the corresponding retro-aldol reaction, but was subject to a different fragmentation pattern wherein cleavage of the C11–C12 and C13–C14 bonds was observed. For example, treatment of closely related hydroxy ester **23** with a strong base resulted in rapid extrusion of isoprene to generate the corresponding keto ester **24** after workup (eq 1).^{29,30} We

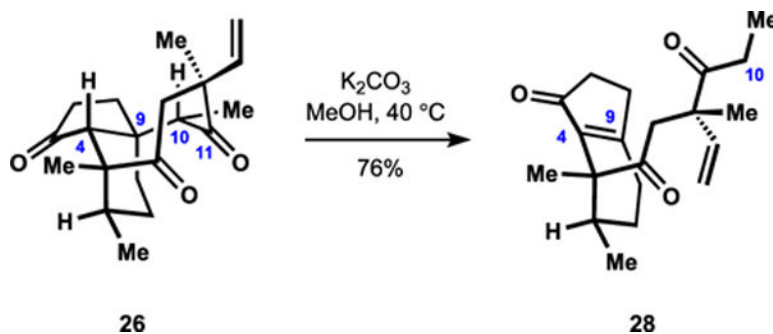


1

eventually found that the carboxyl group at C14 offered a suitable handle en route to the requisite functionalization pattern of the cyclooctane fragment. Thus, formation of trione **26**

upon photocatalyzed oxidation of acid **25** in the presence of acridinium salt **27** provided an encouraging starting point for optimization (entry 1, Table 1).^{31,32} Ultimately, application of iridium complex **17** as a catalyst secured access to product **26** in good yield under optimized conditions (entry 2), where inclusion of TEMPO was critical to achieving high efficiency (cf. entry 3).^{33–35} This transformation likely involves trapping of the intermediate cyclobutyl radical with oxygen or TEMPO and a Criegee- or Grob-type fragmentation to eventually generate the diketone motif.³⁶ Silver(I)-based reagents proved incompetent in the desired oxidation (e.g., entry 4) and instead appeared to preferentially engage the cyclobutanol motif in a cleavage of the C11–C12 bond.³⁷ Application of lead(IV)-based oxidants was similarly unsuccessful (e.g., entry 5).³⁸

Implementation of our oxidative fragmentation tactics in the synthesis involved treatment of silyl ether **15** with a source of fluoride in the presence of hexachloroethane followed by photocatalyzed oxidation of the intermediate carboxylic acid **16** under the optimized conditions.²⁴ Introduction of a chlorine substituent at C4 in triketone **18** provided an important handle for correcting the stereochemical configuration at C10, which proved otherwise challenging in our investigations. Crystallographic studies of triketone **26** revealed antiperiplanar arrangement of the carbonyl at C11 and the adjacent C–H bond in the solid state, which may translate to similar conformational preferences in solution and hinder the requisite deprotonation (see eq 2).²⁴ Indeed, attempted epimerization of substrate **26** invariably resulted in facile retro-Michael fragmentation of the cyclooctanedione motif to deliver tetrahydroindanone **28**.³⁹ Variants of substrate **26** containing a protected cyclopentanone moiety were resistant to enolization at C10 even upon exposure to forcing conditions, as judged by the lack of deuterium incorporation



2

in the presence of isotopically labeled protic solvents. In contrast, subsection of chloroketone **18** to a base in DMSO effected Kornblum oxidation at C2, likely through the intermediacy of the corresponding oxyallyl cation, and enabled in situ epimerization to the desired configuration at C10.⁴⁰ We speculate that formation of the α -hydroxy- α,β -unsaturated ketone retards retro-Michael fragmentation of intermediate **19** due to increased stabilization of the corresponding enolate at C4. Introduction of an sp^2 -hybridized center at C4 may also lead to greater conformational flexibility in the cyclooctanone motif, thereby facilitating

epimerization at C10. Removal of the extraneous carbonyl at C2 was accomplished upon treatment with zinc, and triketone **20** was obtained with the desired configuration at C4.^{41–43}

We found that exposure of penultimate intermediate **20** to sodium in ethanol under carefully controlled conditions resulted in reduction of ketones at C11 and C14, delivering the target compound, mutilin (**2**), in a highly chemo- and stereoselective manner.⁴⁴ The choice of solvent proved critical to success of this transformation, and diminished efficiency and chemoselectivity were observed with other alcohols and in the presence of aprotic cosolvents. Acylation of mutilin (**2**) with acetoxyacetic acid followed by addition of base to the reaction mixture produced pleuromutilin (**1**), completing the synthesis in 16 steps from commercially available material.⁴⁵

In summary, we disclose a new synthetic approach to mutilin antibiotics that relies on ring-expansion of a readily accessible intermediate to establish the requisite tricyclic motif. Our strategy takes advantage of a robust stereochemical relay, which is enabled by the judicious choice of tactics and has led to identification of new reactivity patterns associated with the unique terpenoid core. Other salient features of our approach include an oxidative decarboxylation cascade to access the cyclooctane fragment and a cycloaddition–radical cyclization sequence to rapidly construct the ring-expansion precursor. Application of our strategy to the synthesis of mutilin and pleuromutilin delivers the target compounds in 15 and 16 steps, respectively, from commercially available starting material. Reports of modifications within the terpenoid motif that impart a promising, extended spectrum antibacterial activity to mutilin derivatives suggest that lessons learned during this study may contribute to the development of new leads in the arsenal of antibiotics.

Supplementary Material

Refer to Web version on PubMed Central for supplementary material.

ACKNOWLEDGMENTS

Financial support from the National Institutes of Health (R01GM121678), the University of California, Irvine, and Amgen is gratefully acknowledged. We thank Professor Scott Rychnovsky for guidance and assistance with our computational studies. We also thank Professors Larry Overman and Chris Vanderwal for routine access to their instrumentation and helpful discussions.

REFERENCES

- (1). Kavanagh F; Hervey A; Robbins WJ Antibiotic substances from basidiomycetes. VIII. Pleurotus mutilus (Fr.) sacc. and Pleurotus passeckerianus pilat. Proc. Natl. Acad. Sci. U.S.A 1951, 37, 570. [PubMed: 16589015]
- (2). Poulsen SM; Karlsson M; Johansson LB; Vester B The pleuromutilin drugs tiamulin and valnemulin bind to the RNA at the peptidyl transferase centre on the ribosome. Mol. Microbiol 2001, 41, 1091. [PubMed: 11555289]
- (3). Davidovich C; Bashan A; Auerbach-Nevo T; Yaggie RD; Gontarek RR; Yonath A Induced-fit tightens pleuromutilins binding to ribosomes and remote interactions enable their selectivity. Proc. Natl. Acad. Sci. U.S.A 2007, 104, 4291. [PubMed: 17360517]
- (4). Paukner S; Riedl R Pleuromutilins: Potent drugs for resistant bugs—mode of action and resistance. Cold Spring Harb. Perspect. Med 2017, 7, a027110. [PubMed: 27742734]

- (5). (a) Anchel M Chemical studies with pleuromutilin. *J. Biol. Chem* 1952, 199, 133. [PubMed: 12999825] (b) Arigoni D Structure of a new type of terpene. *Gazz. Chim. Ital* 1962, 92, 884. (c) Birch AJ; Holzapfel CW; Rickards RW The structure and some aspects of the biosynthesis of pleuromutilin. *Tetrahedron* 1966, 22, 359. For X-ray crystallographic studies see: (d) Dobler M; Duerr BG Mono-O-bromoacetylpleuromutilin. *Cryst. Struct. Comm* 1975, 4, 259.
- (6). For isolation of mutilin from fermentation broths see: Knauseder F; Brandl E Pleuromutilins fermentation, structure and biosynthesis. *J. Antibiot* 1976, 29, 125.
- (7). See ref 5b for positional numbering in pleuromutilin. The same numbering is adopted for all intermediates
- (8). Egger H; Reinshagen H New pleuromutilin derivatives with enhanced antimicrobial activity. *J. Antibiot* 1976, 29, 923.
- (9). Daum RS; Kar S; Kirkpatrick P Retapamulin. *Nat. Rev. Drug Discovery* 2007, 6, 865.
- (10). Chahine EB; Sucher AJ Lefamulin: the first systemic pleuromutilin antibiotic. *Ann. Pharmacother* 2020, 54, 1203. [PubMed: 32493034]
- (11). (a). Fazakerley NJ; Procter DJ Synthesis and synthetic chemistry of pleuromutilin. *Tetrahedron* 2014, 70, 6911. (b) Goethe O; Heuer A; Ma X; Wang Z; Herzon SB Antibacterial properties and clinical potential of pleuromutilins. *Nat. Prod. Rep* 2019, 36, 220. [PubMed: 29979463]
- (12). Thirring K; Heilmayer W; Riedl R; Kollmann H; Ivezic-Schoenfeld Z; Wicha W; Paukner S; Strickmann D 12-epi pleuromutilins. *WO2015110481A1*, July 30, 2015.
- (13). For syntheses of pleuromutilin see: (a) Gibbons EG Total synthesis of (\pm)-pleuromutilin. *J. Am. Chem. Soc* 1982, 104, 1767. (b) Boeckman RK Jr.; Springer DM; Alessi TR Synthetic studies directed toward naturally occurring cyclooctanoids. 2. Stereocontrolled assembly of (\pm)-pleuromutilin via a remarkable sterically demanding oxy-Cope rearrangement. *J. Am. Chem. Soc* 1989, 111, 8284. (c) Fazakerley NJ; Helm MD; Procter DJ Total synthesis of (+)-pleuromutilin. *Chem. – Eur. J* 2013, 19, 6718. [PubMed: 23589420] (d) Murphy SK; Zeng M; Herzon SB A modular and enantioselective synthesis of the pleuromutilin antibiotics. *Science* 2017, 356, 956. [PubMed: 28572392] (e) Zeng M; Murphy SK; Herzon SB Development of a modular synthetic route to (+)-pleuromutilin and (+)-12-epi-mutilins, and related structures. *J. Am. Chem. Soc* 2017, 139, 16377. [PubMed: 29048164] (f) Farney EP; Feng SS; Schäfers F; Reisman SE Total synthesis of (+)-pleuromutilin. *J. Am. Chem. Soc* 2018, 140, 1267. [PubMed: 29323492]
- (14). For synthetic studies toward pleuromutilin see: (a) Paquette LA; Wiedeman PE A relay approach to (+)-pleuromutilin. I. De novo synthesis of a levorotatory tricyclic lactone subunit. *Tetrahedron Lett* 1985, 26, 1603. (b) Paquette LA; Bulman-Page PC A relay approach to (+)-pleuromutilin. II. Preparation of an advanced optically pure intermediate. *Tetrahedron Lett* 1985, 26, 1607. (c) Paquette LA; Wiedeman PE; Bulman-Page PC A relay approach to (+)-pleuromutilin. III. Direct degradation of the natural product to the key diketone intermediate and its chemospecific functionalization. *Tetrahedron Lett* 1985, 26, 1611. (d) Paquette LA; Wiedeman PE; Bulman-Page PC (+)-Pleuromutilin synthetic studies. Degradative and de novo acquisition of a levorotatory tricyclic lactone subunit. *J. Org. Chem* 1988, 53, 1441. (e) Paquette LA; Bulman-Page PC; Pansegrau PD; Wiedeman PE (+)-Pleuromutilin synthetic studies. Direct degradation to and independent preparation of an advanced diketone intermediate. Demonstration that reconstruction of the eight-membered ring suffers from serious kinetic retardation. *J. Org. Chem* 1988, 53, 1450. (f) Paquette LA; Pansegrau PD; Wiedeman PE; Springer JP (+)-Pleuromutilin synthetic studies. Examples of intramolecular hydrogen abstraction by the β -carbon of a 2-cyclopentenone subunit with resultant α -coupling. *J. Org. Chem* 1988, 53, 1461. (g) Bacque E; Patrat F; Zard S A concise synthesis of the tricyclic skeleton of pleuromutilin and a new approach to cycloheptenes. *Org. Lett* 2003, 5, 325. [PubMed: 12556183] (h) Lotesta SD; Liu J; Yates EV; Krieger I; Sacchetti JC; Freundlich JS; Sorensen EJ Expanding the pleuromutilin class of antibiotics by *de novo* chemical synthesis. *Chem. Sci* 2011, 2, 1258. [PubMed: 21874155] (i) Liu J; Lotesta SD; Sorensen EJ A concise synthesis of the molecular framework of pleuromutilin. *Chem. Commun* 2011, 47, 1500. (j) Helm MD; Da Silva M; Sucunza D; Findley TJK; Procter DJ A dialdehyde cyclization cascade: an approach to pleuromutilin. *Angew. Chem., Int. Ed* 2009, 48, 9315.
- (15). For examples of epimerization at C4 see: (a) Birch AJ; Cameron DW; Holzapfel CW; Rickards RW Diterpenoid nature of pleuromutilin. *Chem. Ind* 1963, 1963, 374. (b) Berner H; Schulz

G; Schneider H Synthese ab-trans-anellierter derivate des tricyclischen diterpens pleuromutilin durch intramolekulare 1,5-hydrid-verschiebung. *Tetrahedron* 1980, 36, 1807. See also ref 5c.

- (16). For the use of alkylaluminum triflimides as catalysts in hindered Diels–Alder cycloadditions see: Jung ME; Guzaev M Trimethylaluminum–triflimide complexes for the catalysis of highly hindered Diels–Alder reactions. *Org. Lett* 2012, 14, 5169. [PubMed: 23030499]
- (17). Neither methylaluminum triflimide nor the silyl triflate induced the desired reactivity when employed as a sole catalyst For examples of relevant catalysis by Lewis acid-assisted Lewis acids see:(a) Jewett JC; Rawal VH Total synthesis of pederin. *Angew. Chem., Int. Ed* 2007, 46, 6502.For a relevant review see: (b) Yamamoto H; Futatsugi K Designer acids’’: combined acid catalysis for asymmetric synthesis. *Angew. Chem., Int. Ed* 2005, 44, 1924.
- (18). For examples of relevant exo-selective cycloadditions see: (a) Jung ME; Davidov P Efficient synthesis of a tricyclic BCD analogue of ouabain: Lewis acid catalyzed Diels–Alder reactions of sterically hindered systems. *Angew. Chem., Int. Ed* 2002, 41, 4125.For relevant mechanistic considerations see: (b) Lam Y; Cheong PH-Y; Mata JMB; Stanway SJ; Gouverneur V; Houk KN Diels–Alder exo selectivity in terminal-substituted dienes and dienophiles: experimental discoveries and computational explanations. *J. Am. Chem. Soc* 2009, 131, 1947. [PubMed: 19154113]
- (19). Evans PA; Longmire JM; Modi DP Regioselective preparation of α,β -unsaturated ketones via the direct dehydrogenation of triisopropylsilyl enol ethers. *Tetrahedron Lett* 1995, 36, 3985.
- (20). (a) Lo JC; Yabe Y; Baran PS A practical and catalytic reductive olefin coupling. *J. Am. Chem. Soc* 2014, 136, 1304. [PubMed: 24428607] (b) Lo JC; Gui J; Yabe Y; Pan C-M; Baran PS Functionalized olefin cross-coupling to construct carbon–carbon bonds. *Nature* 2014, 516, 343. [PubMed: 25519131] (c) Lo JC; Kim D; Pan C-M; Edwards JT; Yabe Y; Gui J; Qin T; Gutiérrez S; Giacoboni J; Smith MW; Holland PL; Baran PS Fe-catalyzed C–C bond construction from olefins and radicals. *J. Am. Chem. Soc* 2017, 139, 2484. [PubMed: 28094980] (d) Kim D; Rahaman SMW; Mercado BQ; Poli R; Holland P Roles of iron complexes in catalytic radical alkene cross-coupling: a computational and mechanistic study. *J. Am. Chem. Soc* 2019, 141, 7473. [PubMed: 31025567]
- (21). For examples of application in synthesis see: (a) George DT; Kuenstner EJ; Pronin SV A concise approach to paxilline indole diterpenes. *J. Am. Chem. Soc* 2015, 137, 15410. [PubMed: 26593869] (b) Deng H; Cao W; Liu R; Zhang Y; Liu B Asymmetric total synthesis of hispidanin A. *Angew. Chem., Int. Ed* 2017, 56, 5849.(c) Lu Z; Zhang X; Guo Z; Chen Y; Mu T; Li A Total synthesis of aplysiasecosterol A. *J. Am. Chem. Soc* 2018, 140, 9211. [PubMed: 29939021] (d) Godfrey NA; Schatz DJ; Pronin SV Twelve-step asymmetric synthesis of (–)-nodulisporic acid. *J. Am. Chem. Soc* 2018, 140, 12770. [PubMed: 30261724] (e) Thomas WP; Schatz DJ; George DT; Pronin SV A radical-polar crossover annulation to access terpenoid motifs. *J. Am. Chem. Soc* 2019, 141, 12246. [PubMed: 31329434] (f) Xu G; Wu J; Li L; Lu Y; Li C Total synthesis of (–)-daphnezomines A and B. *J. Am. Chem. Soc* 2020, 142, 15240. [PubMed: 32813976] (g) Thomas WP; Pronin SV A concise enantioselective approach to quassinoids. *J. Am. Chem. Soc* 2022, 144, 118. [PubMed: 34958202]
- (22). Obradors C; Martinez RM; Shenvi RA Ph(*i*-PrO)SiH₂: an exceptional reductant for metal-catalyzed hydrogen atom transfers. *J. Am. Chem. Soc* 2016, 138, 4962. [PubMed: 26984323]
- (23). For a review of HAT-initiated reactions see: Crossley SWM; Martinez RM; Obradors C; Shenvi RA Mn, Fe, and Co-catalyzed radical hydrofunctionalizations of olefins. *Chem. Rev* 2016, 116, 8912. [PubMed: 27461578]
- (24). See Supporting Information for X-ray crystallographic analysis
- (25). Deprotonation and silylation of intermediate 9 proceeds at C2 and requires isomerization to the requisite enoxysilane at C4. See Supporting Information for details
- (26). For a relevant cyclization see: (a) Morlender-Vais N; Solodovnikova N; Marek I Intramolecular carbometalation of functionalized terminal alkynes via low-valent titanium complexes. *Chem. Commun* 2000, 2000, 1849.For a relevant review see: (b) Sato F; Urabe H; Okamoto S Synthesis of organotitanium complexes from alkenes and alkynes and their synthetic applications. *Chem. Rev* 2000, 100, 2835–2886. [PubMed: 11749307] For relevant applications in synthesis see: (c) Belardi JK; Micalizio GC Total synthesis of macbecin I. *Angew. Chem., Int. Ed* 2008,

- 47, 4005.(d) Du K; Kier MJ; Stempel ZD; Jeso V; Rheingold AL; Micalizio GC Synthesis of anhydroryanodol. *J. Am. Chem. Soc* 2020, 142, 12937. [PubMed: 32609506]
- (27). a Ketene silyl acetal 14 was obtained as a 14:1 mixture of stereoisomers at the newly formed C–C double bond. The configuration of the major isomer was determined by 2D 1H NMR analysis.
b Precise control over the amount of added base was necessary and accomplished by employing 9-methylfluorene as an indicator. See the Supporting Information for details.
- (28). In the case of enols 21 and 22, the lowest energy conformers that could be expected to offer opposite facial selectivity during electrophilic attack at C12 of the ones depicted in Figure 2 were computed to be 4.67 and 1.68 kcal/mol higher in energy, respectively See the Supporting Information for details.
- (29). Hydroxy ester 23 was prepared from an analogue of intermediate 15 See the Supporting Information for details.
- (30). For a relevant fragmentation of an arylcyclobutanol see: Cohen T; Bhupathy M; Matz JR A practical method for using alkoxide-accelerated vinylcyclobutane ring expansions in the synthesis of six-membered rings. Unexpected orbital symmetry allowed and forbidden 1,3-sigmatropic rearrangements. *J. Am. Chem. Soc* 1983, 105, 520.
- (31). Acid 25 was prepared from intermediate 15 See the Supporting Information for details.
- (32). For relevant examples of photocatalytic decarboxylative hydroxylation in the presence of acridinium salts see: (a) Song H-T; Ding W; Zhou Q-Q; Liu J; Lu L-Q; Xiao W-J Photocatalytic decarboxylative hydroxylation of carboxylic acids driven by visible light and using molecular oxygen. *J. Org. Chem* 2016, 81, 7250. [PubMed: 27385267] See also: (b) Okada K; Okubo K; Oda M Decarboxylative photooxygenation of carboxylic acids by the use of acridine. *Tetrahedron Lett* 1992, 33, 83.
- (33). For relevant examples of photocatalytic decarboxylative hydroxylation in the presence of iridium complexes see: Khan SN; Zaman MK; Li R; Sun Z A general method for photocatalytic decarboxylative hydroxylation of carboxylic acids. *J. Org. Chem* 2020, 85, 5019. [PubMed: 32133856]
- (34). For recent examples of relevant decarboxylative C–O bond formation see: (a) Sakakibara Y; Ito E; Fukushima T; Murakami K; Itami K Late-stage functionalization of arylacetic acids by photoredox-catalyzed decarboxylative carbon-heteroatom bond formation. *Chem.—Eur. J* 2018, 24, 9254. [PubMed: 29718551] (b) Xiang J; Shang M; Lundberg H; Reisberg SH; Chen M; Mykhailiuk P; Beutner G; Collins MR; Davies A; Del Bel M; Gallego GM; Spangler JE; Starr J; Yang S; Blackmond DG; Baran PS Hindered dialkyl ether synthesis with electrogenerated carbocations. *Nature* 2019, 573, 398. [PubMed: 31501569] (c) Li P; Zbieg JR; Terrett JA A platform for decarboxylative couplings via photoredox catalysis: direct access to carbocations from carboxylic acids for carbon-oxygen bond formation. *ACS Catal* 2021, 11, 10997.(d) Li QY; Gockel SN; Lutovsky GA; DeGlopper KS; Baldwin NJ; Bundesmann MW; Tucker JW; Bagley SW; Yoon TP Decarboxylative cross-nucleophile coupling via ligand-to-metal charge transfer photoexcitation of Cu(II) carboxylates. *Nat. Chem* 2022, 14, 94. [PubMed: 34987174]
- (35). For relevant reviews see: (a) Xuan J; Zhang Z-G; Xiao W-J Visible-light-induced decarboxylative functionalization of carboxylic acids and their derivatives. *Angew. Chem., Int. Ed* 2015, 54, 15632.(b) Zeng Z; Feceu A; Sivendran N; Gooßen L Decarboxylation-initiated intermolecular carbon-heteroatom bond formation. *Adv. Synth. Catal* 2021, 363, 2678.
- (36). For trapping of intermediate radicals with TEMPO following decarboxylation see: (a) Cao H; Jiang H; Feng H; Kwan JMC; Liu X; Wu J Photo-induced decarboxylative Heck-type coupling of unactivated aliphatic acids and terminal alkenes in the absence of sacrificial hydrogen acceptors. *J. Am. Chem. Soc* 2018, 140, 16360. [PubMed: 30412399] (b) Wang B; Li P; Miao T; Zou L; Wang L Visible-light induced decarboxylative C2-alkylation of benzothiazoles with carboxylic acids under metal-free conditions. *Org. Biomol. Chem* 2019, 17, 115.(c) Sun L; Zhang Y; Liu J; Li P Visible-light photoredox-catalyzed decarboxylative α -tert-butylation of C(sp³)-H bonds of N-aryltetrahydroisoquinolines with pivalic acid under transition-metal-free conditions. *Synlett* 2021, 32, 993.(d) Wu Z; Gockel SN; Hull KL Anti-Markovnikov hydro(amino)alkylation of vinylarenes via photoredox catalysis. *Nat. Commun* 2021, 12, 5956. [PubMed: 34642311] (e) Song C; Zhang H-H; Yu S Regio- and enantioselective decarboxylative allylic benzylation enabled by dual palladium/photoredox catalysis. *ACS Catal* 2022, 12, 1428.

- (37). For relevant silver-mediated decarboxylations see: (a) Firstad WE; Fry MA; Klang JA Persulfate/silver ion decarboxylation of carboxylic acids. Preparation of alkanes, alkenes, and alcohols. *J. Org. Chem* 1983, 48, 3575. For a relevant review see: (b) Varenikov A; Shapiro E; Gandelman M Decarboxylative halogenation of organic compounds. *Chem. Rev* 2021, 121, 412. [PubMed: 33200917]
- (38). For relevant lead-mediated decarboxylations see: (a) Mosher WA; Kehr CL The decomposition of organic acids in the presence of lead tetraacetate. *J. Am. Chem. Soc* 1953, 75, 3172. (b) Kochi JK The mechanism of oxidative decarboxylation with lead(IV) acetate. *J. Am. Chem. Soc* 1965, 87, 1811. (c) Snider BB; Kwon T Preparation of epoxides by oxidative decarboxylation of β -hydroxy acids. Stereo- and regiochemistry of oxidative elimination of secondary radicals with cupric acetate. *J. Org. Chem* 1990, 55, 1965.
- (39). (a) For the first example of relevant reactivity see: Nägeli, P. Zur Kenntnis des Pleuromutilins. Ph.D. Thesis, ETH, Zurich, 1961. See also refs 14b–e.
- (40). For relevant reactions of oxyallyl cations see: (a) Fort AW Evidence for a delocalized intermediate in the Favorskii rearrangement. 2,6-lutidine-promoted methanolysis of α -chlorodibenzyl ketone. *J. Am. Chem. Soc* 1962, 84, 2620. (b) Föhlisch B; Joachimi R Erzeugung und [4 + 3]-cycloaddition von cyclo-pentenylum-2-olat aus 2-chlorcyclopentanon unter alkoholise-be-dingungen. *Chem. Ber* 1987, 120, 1951. (c) Vander Wal MN; Dilger AK; MacMillan DWC Development of a generic activation mode: nucleophilic α -substitution of ketones via oxy-allyl cations. *Chem. Sci* 2013, 4, 3075.
- (41). Majgier-Baranowska H; Templeton JF Synthesis of steroid 5 α and 5 β 4-ketones from the 4-en-3-one: 1,2-carbonyl transposition. *Tetrahedron* 1999, 55, 3717.
- (42). Freshly activated zinc was required to obtain high diastereoselectivity.
- (43). Intermediate 20 was previously referred to as mutilin trione. See refs 5c and 39a for preparation
- (44). For related reductions of intermediates en route to pleuromutilin see refs 13a and d–f
- (45). The protocol is based on a related procedure reported in ref 13a

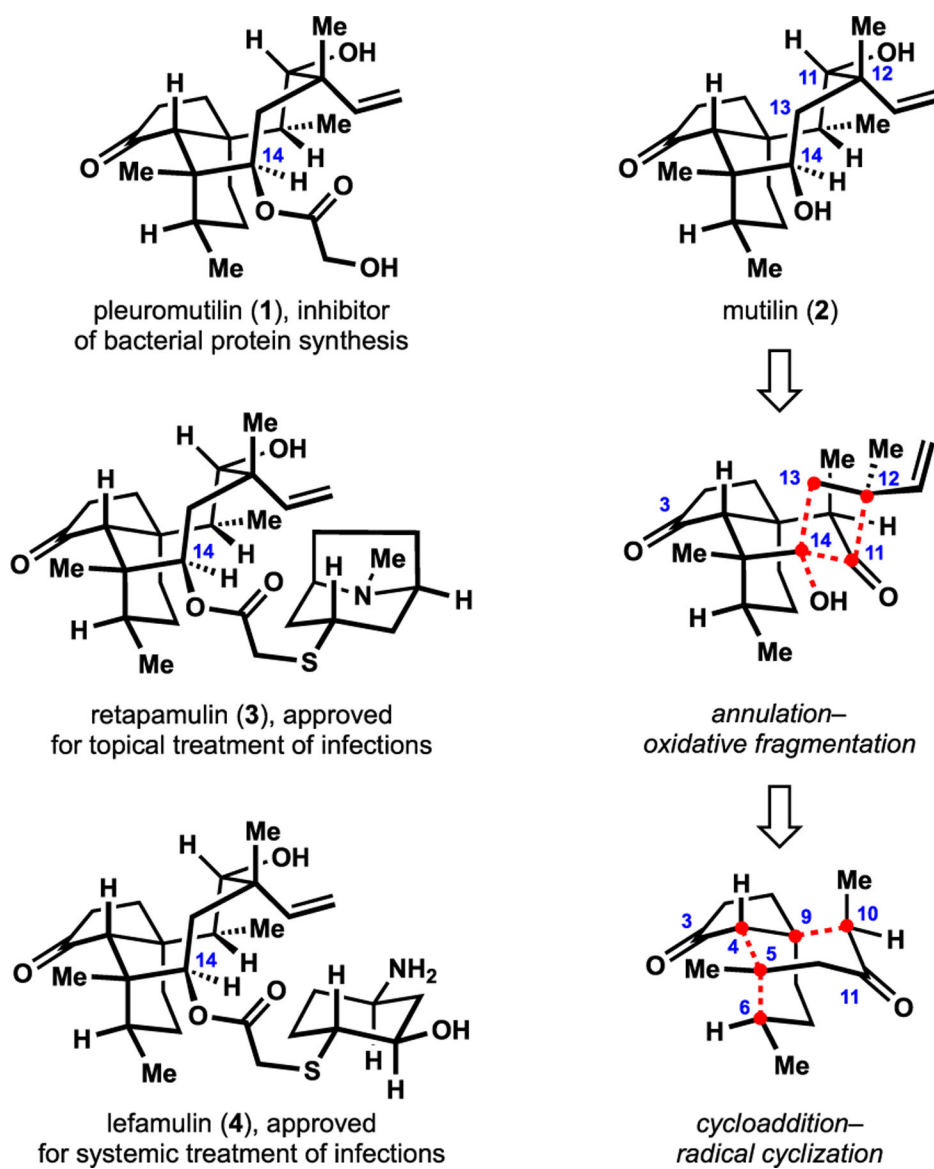


Figure 1. Representative mutilin antibiotics and our approach to the shared tricyclic motif.

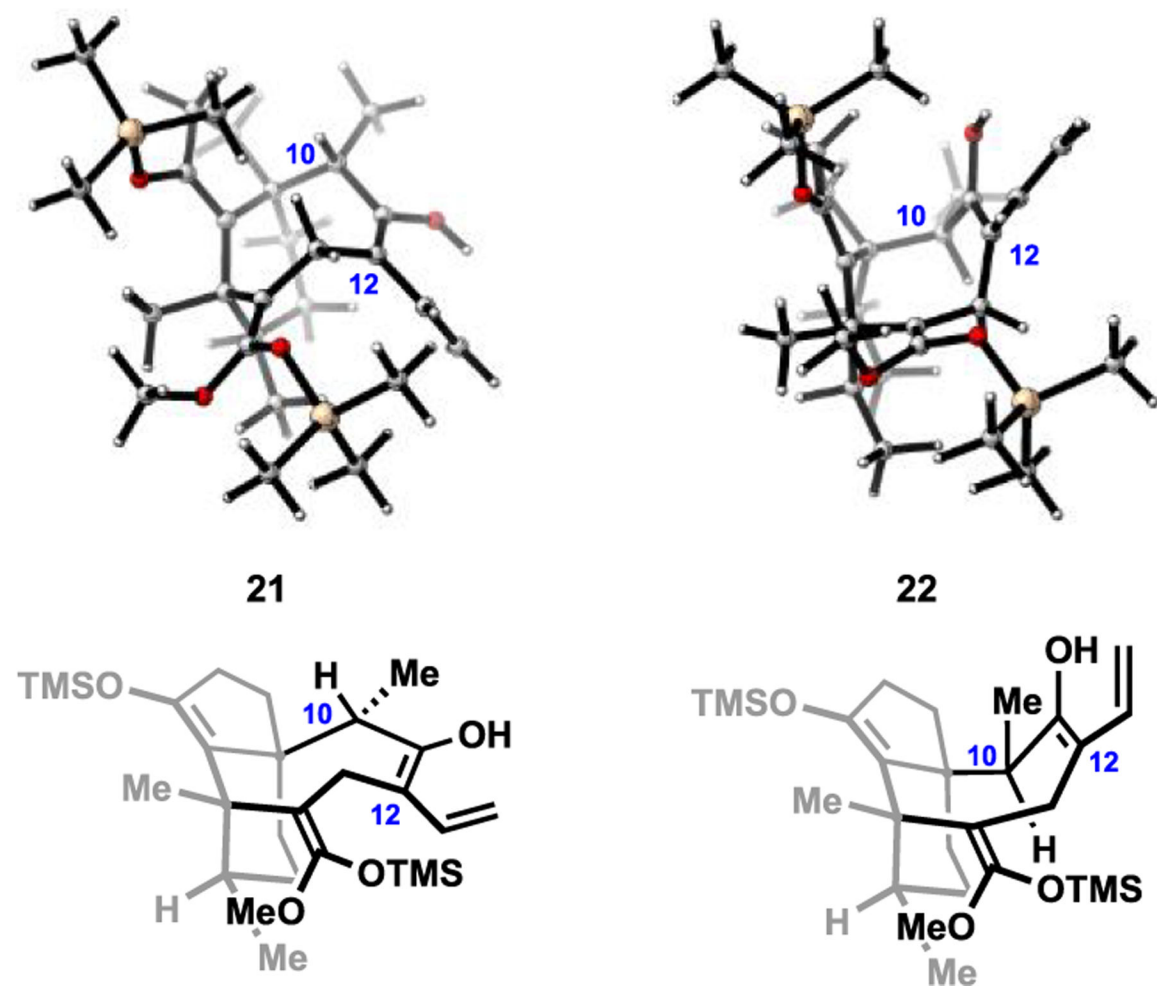
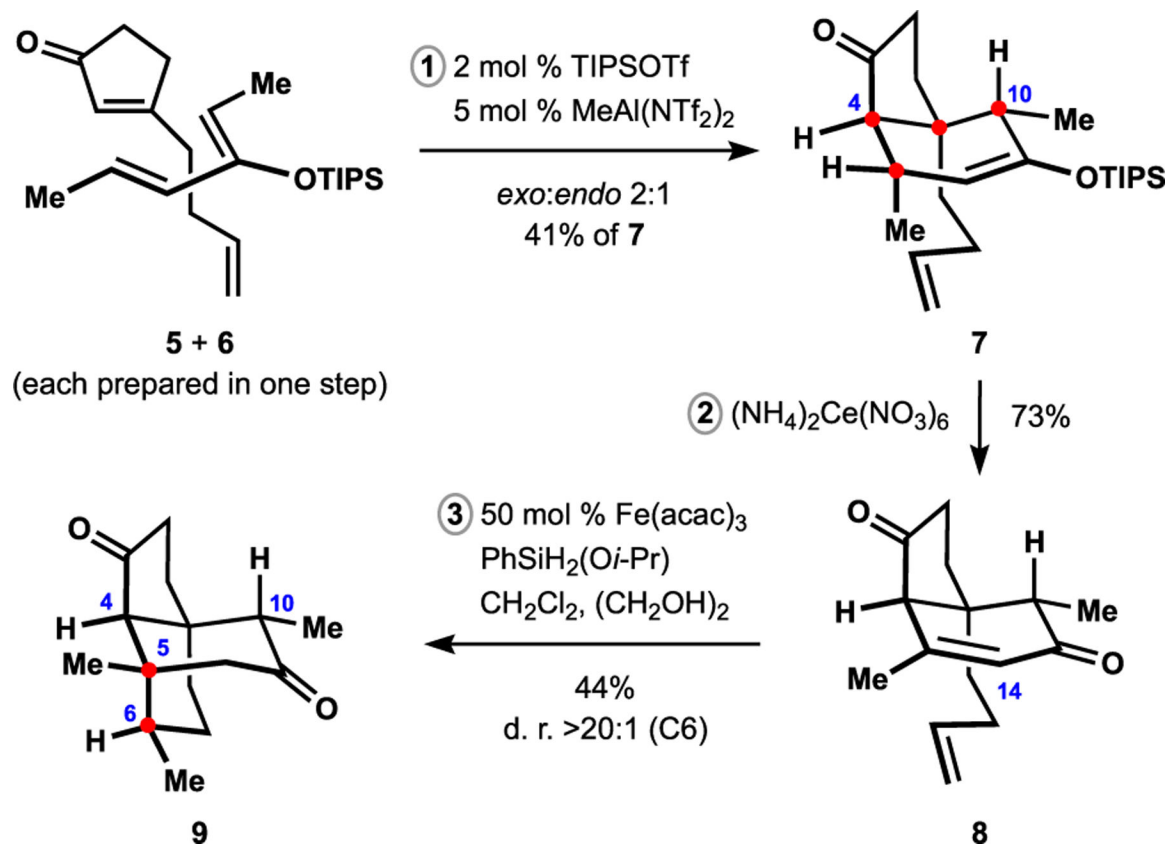
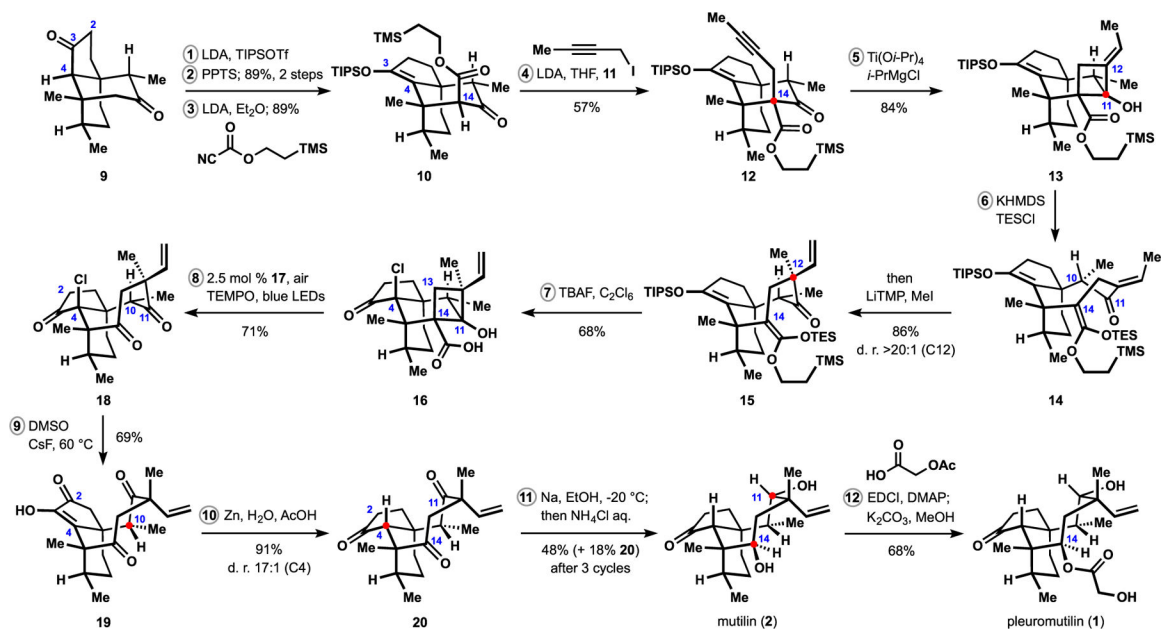


Figure 2. Computed lowest energy conformations of enols **21** and **22**. Computations were performed at the ω B97X-D/6-31G(d) level of theory.



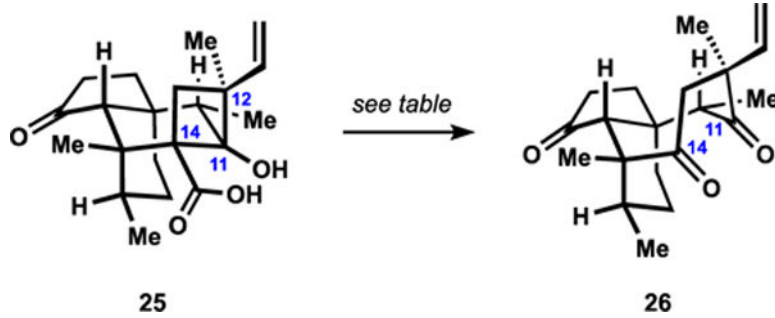
Scheme 1.
Synthesis of Tricyclic Diketone 9



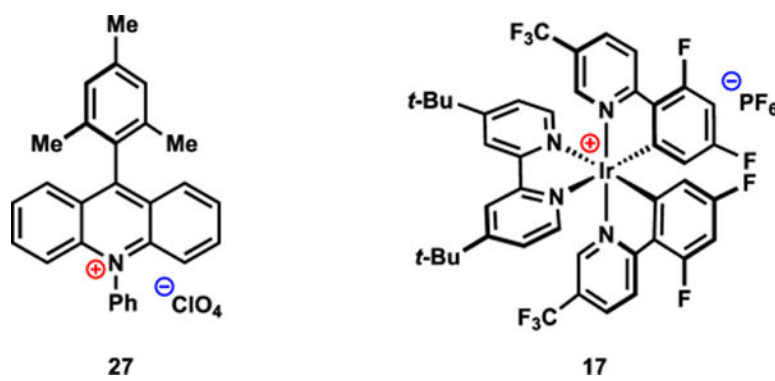
Scheme 2.
Synthesis of Pleuromutilin (1)

Table 1.

Oxidative Decarboxylation en Route to the Desired Functionalization Pattern of the Cyclooctane Fragment



entry	conditions	yield of 26 (%) ^a
1	2.5 mol %, 27 , air, TEMPO, blue LEDs	23
2	2.5 mol % , 17 , air, TEMPO, blue LEDs	80
3	2.5 mol %, 17 , air, blue LEDs	9
4	AgNO ₃ , Me ₂ CO, 60 °C	<5
5	Pb(OAc) ₄ , KOAc, AcOH, 50 °C	<5


^aBased on internal standard and determined by ¹H NMR analysis.